

# Diode-pumped narrow linewidth multi-kW metalized Yb fiber amplifier

CHARLES X. YU,<sup>1\*</sup> OLEG SHATROVOY,<sup>1</sup> T. Y. FAN<sup>1</sup> AND THIERRY F. TAUNAY<sup>2</sup>

<sup>1</sup>MIT Lincoln Laboratory, 244 Wood Street, Lexington, MA 02421

<sup>2</sup>OFS Laboratories, 19 Schoolhouse Road, Somerset, NJ 08873

\*Corresponding author: chars@ll.mit.edu

Received XX Month XXXX; revised XX Month, XXXX; accepted XX Month XXXX; posted XX Month XXXX (Doc. ID XXXXX); published XX Month XXXX

**We investigate high brightness pumping of a multi-kW Yb fiber amplifier in a bi-directional pumping configuration. Each pump outputs 2 kW in a 200  $\mu\text{m}$ , 0.2 NA multi-mode fiber. Gold-coated specialty gain fibers, with 17  $\mu\text{m}$  MFD and 5-dB/meter pump absorption, have been developed. The maximum fiber amplifier output power is 3.1 kW, limited by multi-mode instability, with 90% O-O efficiency and  $M^2 < 1.15$ . The fiber amplifier linewidth is 12 GHz. © 2016 Optical Society of America**

**OCIS codes:** (140.3510) Lasers, fiber; (140.3570) Lasers, single-mode; (140.3615) Lasers, ytterbium; (060.2320) Fiber optics amplifiers and oscillators; (060.2430) Fibers, single-mode.

<http://dx.doi.org/10.1364/OL.99.099999>

Yb-doped fiber laser has experienced exponential growth over the past decade. Currently diode-pumped fiber laser with output power up to 3 kW has been demonstrated [1]. Furthermore, fiber lasers with 10-kW output are commercially available using 1015-nm fiber laser tandem pumping [2]. The output power of a cw Yb fiber laser is limited by stimulated Raman scattering (SRS), as is evident from [1]. Increasing fiber modal area can overcome SRS limitation. However, a larger fiber mode is significantly more susceptible to multi-mode instability (MMI) [3-5], thus degrading the beam quality of the fiber laser output.

Fiber laser power can also be extended via beam combining using coherent beam combining (CBC) and/or wavelength beam combining (WBC) techniques [6-10]. Over the past few years, a number of successful cw beam combining experiments have been performed using kW-class Yb-doped fiber lasers [7, 8]. Presently high-power fiber laser combining efficiencies over 80% have been demonstrated by multiple groups, and the utility of beam combining to extend cw laser power is well established. Because beam-combinable fiber amplifier requires narrow linewidth, its power is limited by stimulated Brillouin scattering (SBS). While a fiber with increased modal area can overcome SBS, lower MMI power threshold associated with a larger fiber mode again degrades the output beam quality, rendering such fibers unsuitable for beam combining [6].

In addition to increasing the fiber modal area, reducing the fiber length is another route to reducing overall fiber nonlinearity for SRS and SBS suppression. Shortening active fiber length while maintaining overall pump absorption for constant modal area requires higher Yb-doping and/or smaller pump clad. While the former is a long-term material research project, rapid improvement in pump brightness makes reducing pump clad a viable option. Over 300 W output power in a 100- $\mu\text{m}$ , 0.22 NA fiber-coupled diode has been reported [11]. Moreover, WBC technique [12] can multiply this pump brightness.

In the case of a short active fiber, thermal management becomes a main challenge. Even though spectroscopic study indicates that active Yb fiber can operate at elevated temperature with minimal loss of efficiency [13], the acrylate coating for pump guiding operates only below 100 °C. In addition to acrylate coating damage,  $dn/dT$  effect becomes significant at high heat loads and modifies fiber refractive index profile (RIP) [14]. Fig. 1 shows quantum-defect heat-load deposition along the length of a bi-directionally pumped 3-kW fiber amplifier similar to the fiber amplifiers investigated in this work. The peak heat loads, in excess of 150 W/m, are near the two fiber ends where the pumps are coupled. Solving the heat equation for a cylindrical fiber shows that  $dn/dT$  due to peak heat load is a significant fraction of the core/clad index difference ( $\Delta n$ ). An increase in  $\Delta n$  between fiber core and cladding increases fiber NA, reduces higher-order-mode (HOM) suppression and lowers the MMI threshold.

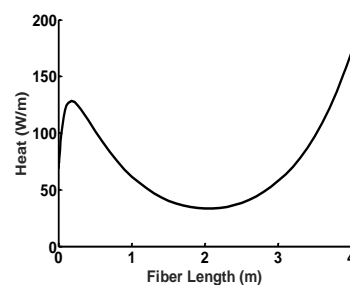


Fig. 1 Sample heat load along fiber amplifier length for bi-directional pumping.

Fig. 2 shows modeled HOM (LP11) loss for a fiber of the same type as the ones used in this Letter. Because our main interest is in the regime with high heat load, we add  $dn/dT$  to the fiber RIP and compute HOM loss based on this modification. Comparing to the room temperature case (0W/m heat load), addition of 150W/m heat load to the fiber degrades LP11 loss by > 100dB. Thus, as fiber amplifier output increases, its HOM suppression degrades and eventually MMI sets in.

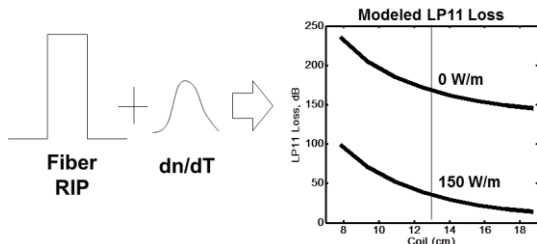


Fig. 2 Modeled LP11 loss per meter vs. coil diameters for 0 W/m and 150 W/m heat loads based on fiber RIP and accounting for  $dn/dT$ ; fiber HOM loss degrades with increased heat load.

LP11 loss can be used to predict the onset of MMI in the regime where effects due to high heat load dominate. According to previous studies [3], HOM experiences very high gain over short interaction length once MMI sets in. Therefore we use the peak heat load in the fiber amplifier when accounting for  $dn/dT$  effects. Based on experiences at various organizations [15], we select 35dB/m HOM loss as MMI threshold. This design rule is used for fiber designs in this Letter.

The experimental setup is shown in Fig. 3. The 976-nm pump lasers are prototypes from Teradiode Inc. Each pump outputs 2 kW in a 200- $\mu$ m, 0.2 NA delivery fiber. Over 90% of the power is within  $\pm 2$ nm of 976 nm. Such record pump brightness is achieved by incorporating WBC technology [12]. The fiber power amplifier is bi-directionally pumped using dichroic mirrors. The pump transmission and signal reflection for these dichroic mirrors are both >99%. We calibrate the residual pump reflections from the dichroic mirrors and use them to monitor the pump power in situ. The coupling lenses for pump and signal are custom fused silica aspherical single-element lenses fabricated using Magnetorheological Finishing (MRF) polishing techniques. We achieve better than 99% pump coupling into the gain fiber cladding using these lenses. Signal coupling into the fiber core is 65% and limited by mode matching. The seed wavelength is 1066 nm and is spectrally broadened using an electro-optic phase modulator for SBS suppression. The RF drive signal for the phase modulator comes from a pseudorandom bit sequence (PRBS) source. The broadened optical seed is then amplified with two IPG pre-amplifiers to achieve output power up to 50 W before it was sent into our fiber amplifier for kW+ output power.

In addition to the glass pump clad, the active fiber has outer-clad made of F-doped glass and protective coating. This triple-clad active fiber is potted in an aluminum v-groove plate using thermally conductive RTV (Dow Corning SE4486). Different v-groove plates are designed for different coil diameters. The two fiber ends are terminated with 2-mm diameter, 5-mm long fused silica endcaps and soldered to aluminum plates. The endcaps are AR-coated for both 976 nm and 1066 nm. The straight fiber section at each fiber end is  $\sim 8$  cm.

The fiber amplifier output is coupled out using the counter-pump dichroic mirror and routed into the diagnostics. In addition to power meter, PER measurement,  $M^2$  meter, CCD beam imager we also use a fiber to measure the on-axis intensity to detect the onset of MMI. While this fiber amplifier does not have a cladding stripper, the cladding light at 1066 nm is <30 W. To protect the pump lasers from residual pump power, we design the fiber amplifier length for > 19 dB pump absorption. This leads to an O-O efficiency of  $\sim 90\%$  for these fiber amplifiers. Furthermore, we found that, while the active fiber is not polarization-maintaining, the fiber modules exhibit large birefringence due to relatively tight fiber coil (12-13 cm) and short fiber length (3-4 meters). The fiber modules have >10 dB PER without active polarization control, and their SBS performance is close to the worst-case polarization. With active polarization control our fiber module PER can be improved to > 18 dB.

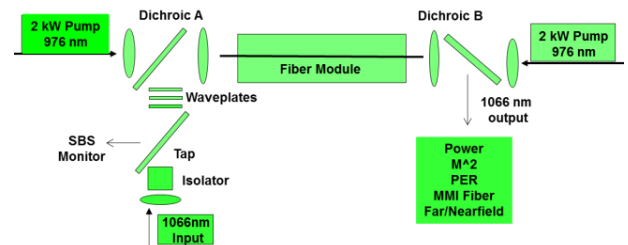


Fig. 3 Experimental Setup: free-space bi-directionally pumped fiber amplifier.

Two triple-clad fiber designs, both with 17- $\mu$ m mode field diameter (MFD), are investigated. The fiber design principle can be found in [16]. An additional modal-filtering feature is added to the step-index fiber design to enhance HOM loss while maintaining ease of splicing to standard step-index fiber. The fiber core designs are the same for the two fibers. However, the modal-filtering features are different to achieve different HOM losses. Both fibers are single-mode at room temperature with a modal cutoff of 1030 nm

To match the 200- $\mu$ m, 0.2 NA pump fibers, the fiber cladding diameters for the two fibers are 180  $\mu$ m while their F-doped outerclads are designed for 0.24 NA. This leads to pump absorption of 5 dB/m at 976 nm. Our fiber amplifier uses 4 meters of active fiber for 20 dB total pump absorption. The first fiber has acrylate coating outside of its F-doped outerclad for protection and handling. The second fiber, designed with larger HOM loss and for higher power operation, has gold coating outside of its F-doped outerclad. Calculation shows that the temperature of the fiber acrylate coating can exceed its long-term damage threshold for high heat load operating regime, as shown in Fig. 4 for our 3-kW case. Gold coating not only can operate at significantly higher temperature, but also provides a thermal ground so that the overall fiber amplifier temperature is lowered.

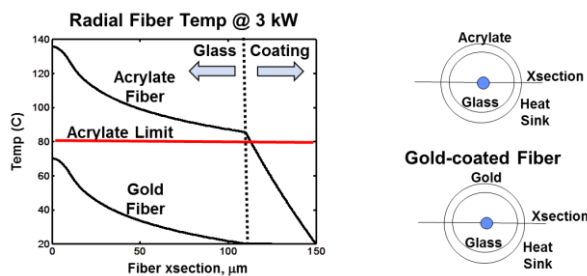


Fig. 4 Calculated radial temperature profile of the active fiber, assuming perfect heat sinking along its periphery.

HOM losses are computed for both fiber designs based on the sum of measured fiber RIP and modeled  $dn/dT$  effects. Based on modeled and measured LP01 loss at room temperature, 13-cm was selected as the coil diameter. Fig. 5 shows the LP11 loss as a function of heat load for the first fiber, which has acrylate coating. HOM loss is  $>150$  dB/m at room temperature but is reduced to  $\sim 35$  dB/m with a heat load of 140 W/meter. This corresponds to the peak heat load for the counter-pumped fiber amplifier case with 1.4 kW of output power. We experimentally confirmed 1.4-kW as the MMI threshold for the counter-pumping case on multiple fiber modules. The MMI threshold for the co-pump case is similar to the counter-pump case. The MMI threshold nearly doubles with bi-directional pumping, to 2.6 kW. This is because bi-directional pumping reduces both  $dn/dT$  and  $\Delta T$  by  $\sim$  a factor of 2 at fixed output power compared with single-side pumping, as illustrated in Fig. 1. Fig. 6a shows the experimental data including co-pumping, counter-pumping and bi-directional pumping cases. The O-O efficiencies for all three cases are 90%. The  $M^2$  for all the cases is  $< 1.15$  up to 2.5 kW of output power. Without active polarization control, the output PER is 12 dB. Fig. 6b shows the OSA spectrum containing both backward Rayleigh and SBS signals at 2.1 kW. With a 10 GHz PRBS-8 signal, the SBS signal is still well below the Rayleigh backscatter. We used 12 GHz PRBS-8 input to seed the 2.5 kW fiber amplifier output.

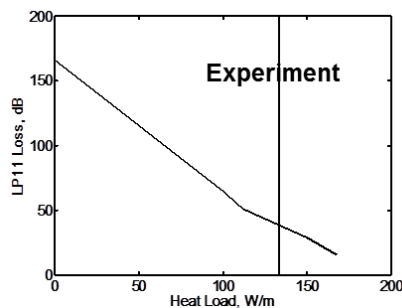


Fig. 5 Modeled LP11 loss as a function of fiber peak heat load at 13-cm coil diameter for first fiber. Experiment verified our design rule of using 35 dB/m HOM loss as MMI threshold.

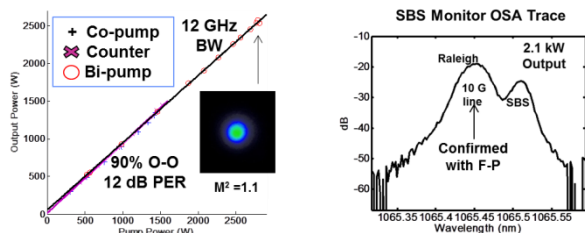


Fig. 6 Experimental results for first fiber (a) Pump vs. output for co-pumping, counter-pumping and bi-directional pumping (b) Backward Rayleigh scattering and SBS at 2.1 kW.

Fig. 7 shows the LP11 loss as a function of heat load for the second fiber, which has gold-coating. HOM loss is  $>700$  dB/m at room temperature but is reduced to  $\sim 35$  dB/m with a heat load of 170 W/meter. This corresponds to the peak heat load for the counter-pumped fiber amplifier case with 1.7 kW of output power. Experiment confirmed 1.7 kW as MMI power threshold. The MMI threshold for the co-pump case is similar to the counter-pump case. The MMI threshold nearly doubles with bi-directional pumping, to 3.2 kW. Fig. 8a shows the pump vs. output for bi-directional pumping. The O-O efficiency is 90% up to 3.1 kW and  $M^2$  is  $< 1.15$  at 3 kW. Without active polarization control, the output PER is 10 dB. Fig. 8b shows the spectrum containing both backward Rayleigh and SBS signals at 3 kW. With a 12.5 GHz PRBS-8 signal, the SBS signal is slightly below the Rayleigh backscatter.

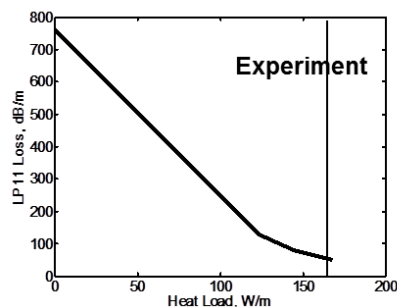


Fig. 7 Modeled LP11 loss as a function of fiber peak heat load at 13-cm coil diameter for second fiber. Experiment verified our design rule of using 35 dB/m HOM loss as MMI threshold.

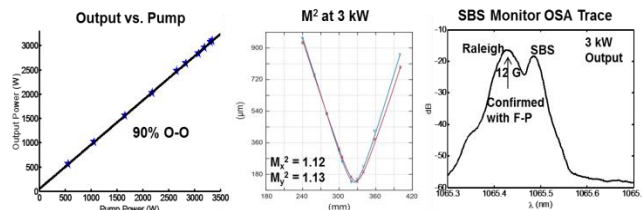


Fig. 8 Experimental results for second fiber (a) Pump vs. output for bi-directional pumping and  $M^2$  at 3 kW (b) Backward Rayleigh scattering and SBS at 3 kW.

In summary, we have demonstrated a linearly polarized, diffraction-limited 3.1-kW fiber amplifier with 90% O-O efficiency and 12 GHz linewidth. This achievement is enabled by utilizing short active fiber with record brightness 976-nm pump lasers. We devised a design rule for MMI-free operation in the high heat load regime. This simple design rule is validated with specialty fiber that can operate MMI-free with 170 W/m of heat load. The ability to handle such high heat load allows future multi-kW power scaling with direct diode pumping at 976 nm.

**Funding.** DARPA/MTO, PM Joseph Mangano

**Acknowledgment.** We would like to thank Mike Cruz for furnishing and repairing the high brightness pump lasers and Jason Langseth and Steve Augst for assistance with modelling.

*This material is based upon work supported by the Defense Advanced Research Projects Agency under Air Force Contract No. FA8721-05-C-0002 and/or FA8702-15-D-0001. Any opinions, findings, conclusions or recommendations expressed in this material are those of the author(s) and do not necessarily reflect the views of the Defense Advanced Research Projects Agency.*

## References

1. V. Khitrov, J. Minelly, R. Tumminelli, V. Petit, E. Pooler, Proc. SPIE 8961, 896120V (2014).
2. E. Stiles, in Proceedings of the 5th International Workshop on Fiber Lasers (2009).
3. A. Smith, and J. Smith, Opt. Exp., 19(11), 10180 (2011).
4. B. Ward, C. Robin, and I. Dajani, Opt. Exp., 20(10), 11407 (2012).
5. M. Karow, H. Tünnermann, J. Neumann, D. Kracht, and P. Webels, Opt. Lett., 37(20), 4242 (2012).
6. C. X. Yu and T. Y. Fan, in High-power laser handbook, The McGraw-Hill Companies, New York, 533-571 (2011).
7. C. X. Yu, S. Augst, S. M. Redmond, K. Goldizen, D. Murphy, A. Sanchez, and T. Y. Fan, Opt. Lett., 36(14), 2686 (2011).
8. G. Goodno, S. McNaught, J. E. Rothenberg, T. McComb, P. Thielen, M. Wickham and M. Weber, Opt. Lett., 35(10), 1542 (2010).
9. S. J. Augst, J. Ranka, T. Y. Fan, and A. Sanchez, J. Opt. Soc. Am. B., 24(8), 1707 (2007).
10. E. Honea, R. Afzal, M. Savage-Leuchs, J. Henrie, K. Brar, N. Kurz, D. Jander, N. Gitkind, D. Hu, C. Robin, A. Jones, R. Kasinadhuni, R. Humphreys, Proc. SPIE. 9730, 97300Y (2016).
11. Y. Kasai, S. Sakamoto, Y. Takahashi, K. Katagiri, Y. Yamagata, A. Sakamoto, D. Tanaka, Proc. SPIE 9733, 973309 (2016).
12. B. Chann, A. Goyal, A. Sanchez, T. Y. Fan, B. Volodin, and V. Ban, Opt. Lett., 31(9), 1253 (2006).
13. T. Newell, P. Peterson, A. Gavrielides and M. Sharma, Opt. Comm., 273(1), 256 (2007).
14. D. Brown, and H. Hoffman, IEEE J. Quant. Electron., 37(2), 207 (2001)
15. MIT Lincoln Lab, private conversation; Nufern, private conversation; OFS, private conversation.
16. T. Taunay, US Patent 9366806 B2 (2016).

# References

1. Khitrov, V., Minelly J., Tumminelli, R., Petit, V., Pooler E. S., "3kW single-mode direct diode-pumped fiber laser," Proc. SPIE 8961, 896120V(2014).
2. Stiles, E., "New developments in IPG fiber laser technology," in Proceedings of the 5th International Workshop on Fiber Lasers (2009).
3. Smith, A., and Smith, J., "Mode Instability in high power fiber amplifiers," Opt. Exp., 19(11), 10180 (2011).
4. Ward, B., Robin, C., and Dajani, I., "Origin of thermal modal instability in large mode area fiber amplifiers," Opt. Exp., 20(10), 11407 (2012).
5. Karow, M., Tünnermann H., Neumann J., Kracht D., and Webels, P., "Beam quality degradation of a single-frequency Yb-doped photonic crystal fiber amplifier with low mode instability threshold power," Opt. Lett., 37(20), 4242 (2012).
6. Yu, C. X. and Fan, T. Y., [High-power laser handbook], The McGraw-Hill Companies, New York, 533-571 (2011).
7. Yu, C. X., Augst, S., Redmond, S. M., Goldizen, K., Murphy, D., Sanchez, A. and Fan, T. Y., "Coherent combining of a 4 kW, eight-element fiber amplifier array," Opt. Lett., 36(14), 2686 (2011).
8. Goodno, G., McNaught, S., Rothenberg, J. E., McComb, T., Thielen, P., Wickham, M. and Weber, M. E., "Active phase and polarization locking of a 1.4 kW fiber amplifier," Opt. Lett., 35(10), 1542 (2010).
9. Augst, S., Ranka, J., Fan, T. Y., and Sanchez, A., "Beam combining of Yb fiber amplifiers," J. Opt. Soc. Am. B., 24(8), 1707 (2007).
10. Honea, E., Afzal, R., Savage-Leuchs, M., Henrie, J., Brar, K., Kurz, N., Jander, D., Gitkind, N., Hu, D., Robin, C., Jones, A., Kasinadhuni, R., Humphreys, R., "Advances in fiber laser spectral beam combining for power scaling," Proc. SPIE. 9730, 97300Y (2016).
11. Kasai, Y., Sakamoto, S., Takahashi, Y., Katagiri, K., Yamagata, Y., Sakamoto, A., Tanaka D., "High-brightness laser diode module over 300W with 100 $\mu$ m/NA 0.22 fiber," Proc. SPIE 9733, 973309 (2016).
12. Chann, B., Goyal, A., Sanchez, A., Fan, T. Y., Volodin, B., and Ban, V., "Efficient, high-brightness wavelength-beam-combined commercial off-the-shelf diode stacks achieved by use of a wavelength-chirped volume Bragg grating," Opt. Lett., 31(9), 1253 (2006).
13. T. Newell, P. Peterson, A. Gavrielides and M. Sharma, "Temperature effects on the emission properties of Yb-doped optical fibers," Opt. Comm., 273(1), 256 (2007).
14. Brown, D. and Hoffman, H., "Thermal, stress, and thermo-optic effects in high average power double-clad silica fiber lasers," IEEE J. Quant. Electron., 37(2), 207 (2001).
15. MIT Lincoln Lab, private conversation; Nufern, private conversation; OFS, private conversation.
16. Taunay, T., "Gain-producing fibers with increased cladding absorption while maintaining single-mode operation," US Patent 9366806 B2 (2016)

